# Aureole Nanofibers by Electrospinning of PAMAM-PEO Solution

**Mohammad Madani, Naser Sharifi-Sanjani, Rasoul Iraji-Rad**

*School of Chemistry, University College of Science, University of Tehran, Tehran, Iran*

Received 31 December 2008; accepted 11 March 2009
DOI 10.1002/app.30401
Published online 1 May 2009 in Wiley InterScience (www.interscience.wiley.com).

**ABSTRACT:** Poly(amido amine) (PAMAM) dendrimer-polyethylene oxide (PEO) nanofibers as dendrimeric-polymeric composite nanofibers were prepared via electrospinning of PEO solution containing PAMAM dendrimer. The resultant fibers were characterized by means of transmission electron microscopy (TEM), differential scanning calorimetry (DSC), and thermogravimetric analysis (TGA). The morphology and thermal properties of PEO nanofibers with and without PAMAM dendrimer were compared and the effect of PAMAM concentration on morphology and thermal properties of the resultant fibers was studied. The fibers had a size range of about 400–1300 nanometer in diameter with aureole morphology in most regions. The phase change temperature, phase transition heat, and the crystallinity of the produced composite fibers were determined by DSC analyses. TGA was also used to confirm the presence of PAMAM and to determine the amount of it within the fibers. © 2009 Wiley Periodicals, Inc. J Appl Polym Sci 113: 3005–3011, 2009

**Key words:** nanocomposites; fibers; dendrimers; aureole morphology; electrospinning

## INTRODUCTION

In the past decade, electrospinning has attracted tremendous interests in the research community simply because it provides a facile and effective means in producing ultrafine fibers with diameters ranging from microns down to a few nanometers. Recently, there has been much interest in extending this technique to produce uniform fibers with novel compositions and morphologies. For example, modification of the spinneret has facilitated the electrospinning of hollow, core-sheath, and porous fibers.[1] The produced electrospun nanofibers have a larger specific surface area and small diameter size compared with conventional nonwoven fabrics. Because of the inherently high aspect ratio and specific surface area, electrospun nanofibers are potentially useful for a variety of applications in diverse areas ranging from membranes and sensors to nanocomposites, nanodevices, and tissue engineering,[2] and numerous researchers have explored electrospinning of polymer solutions that have a solid phase, e.g., particles, carbon nanotubes, or proteins dispersed in them.[3–11] In contrast, there has been no report of electrospinning of polymer solution containing dendrimer. The electrospun mat provides highly porous nanostructure with interconnected pores and extremely large surface area to volume ratio.

To show the ability of dendrimer transportation of the traveling polymer jet in electrospinning, we are reporting preparation of poly(amido amine)-polyethylene oxide (PAMAM-PEO) composite nanofibers through electrospinning.

Dendrimers are morphological architectures different from typical polymers. In the case of poly(amido amine) (PAMAM) dendrimers, the repeating units, consisting of an amido amine, are grown from an ethylene diamine core, and the dendritic structure can be obtained with different terminal groups, such as amine (—$NH_2$), hydroxyl (—OH), and carboxylate (—COO—).[12] Properties and applications of PAMAM dendrimers have extensively been investigated.[13–20]

Kovvali and Sirkar[21,22] recently reported an excellent $CO_2/N_2$ selectivity for the viscous and nonvolatile liquid PAMAM dendrimer as an immobilized liquid membrane at the isobaric test conditions of atmospheric pressure. Interestingly, with the feed containing saturated water vapor, the PAMAM dendrimers showed excellent $CO_2$ selectivity. As such, because exhausted gases usually contain saturated water vapor, this excellent $CO_2$ selectivity would seem to be effective in $CO_2$ separation from fossil fuel emissions. As the PAMAM dendrimer is a liquid, it is necessary to affix PAMAM dendrimer to appropriate support materials, such as polymeric nanofibers. The aim of this study is to report that by adding PAMAM dendrimer in to the PEO solution, aureole nanofibers can be obtained.

*Correspondence to:* M. Madani (mmadani@khayam.ut.ac.ir).

**TABLE I**
**Recipe Used in Preparation of Electrospinning Solution**

| Exp. | PEO concentration (%) | The ratio of PAMAM : PEO |
|---|---|---|
| D1 | 5 | 70 : 30 |
| D2 | 5 | 60 : 40 |
| D3 | 5 | 50 : 50 |
| D4 | 5 | 40 : 60 |
| D5 | 5 | 30 : 70 |
| N | 5 | 0 : 100 |

In this work, dendrimeric (PAMAM)-polymeric (PEO) composite nanofibers were prepared via electrospinning of PEO solution containing various amounts of third generation PAMAM dendrimer. Extensive characterization of fibers was carried out using transmission electron microscopy (TEM), differential scanning calorimetry (DSC), and thermogravimetric analysis (TGA) techniques, and the results were compared with those of the fibers produced in electrospinning of pure PEO solution.

## EXPERIMENTAL

The following six experiments (Exp. D1, D2, D3, D4, D5, and N) that are listed in Table I were carried out. Exp. D1: 0.5 g of PEO (with weight average molecular weight of 900,000 g/mol, supplied by Acros Organics Co.) was added to 10 mL of distilled water containing various amounts (given in Table I) of PAMAM dendrimer (prepared according to Ref. 23) and the mixture was left still for 2 days to obtain a homogenous PEO solution containing PAMAM dendrimer. The polymer–dendrimer solution was put into a hypodermic syringe. A syringe pump (Stoelting Co., USA) was used to feed the polymer solution into a metallic needle with an inner diameter of 0.7 mm. A grounded aluminum foil as collector was placed at a fixed distance of 20 cm from the needle. The feed rate of the syringe pump was fixed at 0.7 mL/h. A positive potential of 18 kV was then applied to the polymer solution using a high voltage power supplier (MH 100 series, HiTek Power Co., UK) with maximum voltage of 50 kV. Electrospun nanofibers were collected on the surface of the grounded aluminum foil.

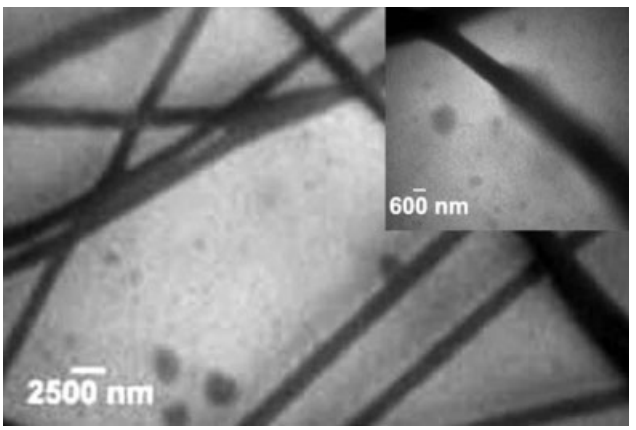


**Figure 1** TEM micrograph of the nanofibers produced in Experiment D1.

Exp. N: To compare with D series experiments, electrospinning of pure PEO solution was also carried out.

A CEM 902A ZEISS transmission electron microscope with an accelerating voltage of 80 kV was used to obtain information about the morphology and size of fibers. The electrospun fibers were directly deposited onto a copper grid and then analyzed by TEM technique. Thermal properties of the electrospun fibers were analyzed by thermogravimetric analysis (Model TGAQ50, TA Instruments) at 20°C/min for heating rate and DSC (Model DSCQ100, TA Instruments) at 10°C/min for heating rate under the inert gas of Ar.

## RESULTS AND DISCUSSION

Figure 1 displays the TEM micrographs of fibers obtained from Exp. D1 (electrospinning of PEO-PAMAM solution having 30 : 70 ratio) and as it shows, the fibers have the size range between 700 and 1300 nm based on TEM micrographs and there is an aureole around the most parts of the fibers, which has produced a special morphology for the nanofibers. This fact is related to the presence of

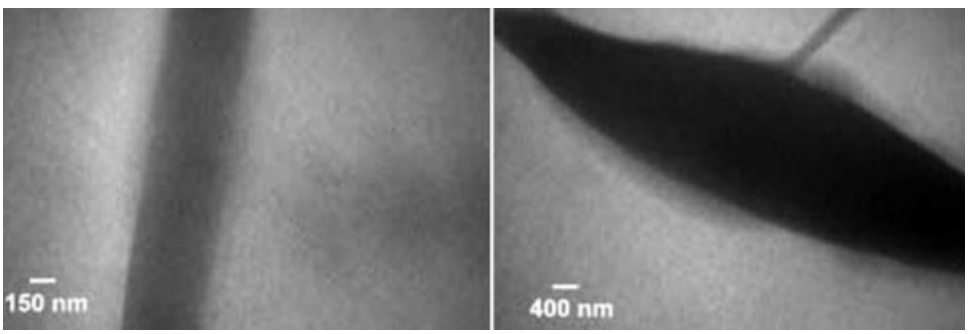


**Figure 2** TEM micrographs of the nanofibers produced in Experiment D3.

PAMAM dendrimer within the fibers that migrate to the surface of the fibers after they are formed and produce nanofibers with the aureole morphology. According to the aforementioned fact, every part of the nanofibers that have more dendrimer show stronger aureole morphology. To explain the influence of PAMAM dendrimer concentration on the morphology of the fibers, a series of experiments were carried out. Figure 2 shows the TEM micrographs of fibers obtained from Exp. D3 (electrospinning of PEO-PAMAM solution having 50 : 50 portion), which show less aureole morphology than D1 fibers due to the lesser amounts of dendrimer within the fibers. This novel morphology for the fibers obtained by electrospinning offers new prospect for the preparation of polymeric nanofibers with new property profiles. In other words, the third generation PAMAM dendrimer has 32 terminal groups, so it increases the number of active terminal groups per unit area, which is useful for chemical sensing applications.

The beads (Fig. 2, on the right) that are produced in some parts of the fibers show aureole morphology stronger than other parts of the fibers because of the higher concentration of the PAMAM within the beads. The fact confirms the role of the PAMAM dendrimer in producing the aureole morphology. Beads are produced due to the low viscosity that gives rise to the jet break at the capillary tip.

The same results can be concluded from Experiment D4 (electrospinning of PEO-PAMAM solution having 60 : 40 ratios). The TEM micrograph of D4 fibers (Fig. 3) shows this aureole morphology in fewer parts compared with previous D fibers due to the decrease in PAMAM concentration in the fibers.

Figure 4 displays the TEM micrographs of the fibers produced in Experiment D5 (electrospinning of PEO-PAMAM solution having 70 : 30 ratio) and as it can be seen, according at the resolution level of the used TEM, there is no significant aureole morphology due to the insufficient amounts of the PAMAM dendrimer within the fibers.

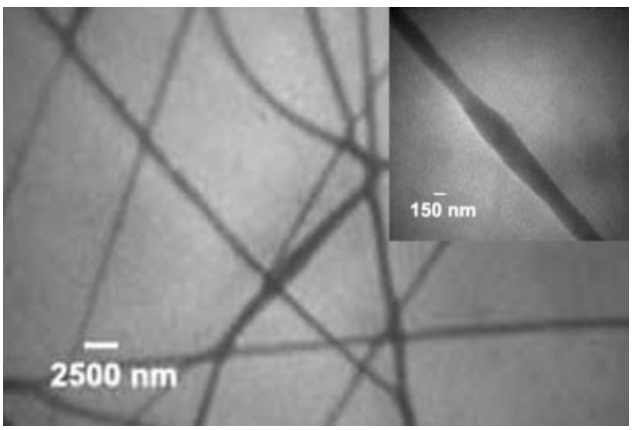


**Figure 4** TEM micrographs of the nanofibers produced in Experiment D5.

Figure 5 displays the TEM micrograph of N fibers (electrospinning of pure PEO solution) and, as it shows and as expected, there is no aureole morphology due to the absence of PAMAM dendrimer. No fibers can be obtained by electrospinning of PEO-PAMAM solution having 20 : 80 ratios due to the low viscosity of the electrospinning solution.

Figure 6 displays the chemical structure of PAMAM dendrimer. The dendrimer size is about 15 Å for G3.[23]

What is the formation mechanism? The highly branched nature of the dendrimer in such systems can result in more complex phase behavior; further complex morphologies may be induced by the presence of a crystallizable PEO. Other researchers indicate that PEO-PAMAM diblocks copolymers exhibit segregation when spread as monolayers at the air–water interface,[23–25] and also exhibit microphase segregation in the bulk state.[24,25] The formation mechanism of the aureole morphology and the role of dendrimer in this work could be related to the

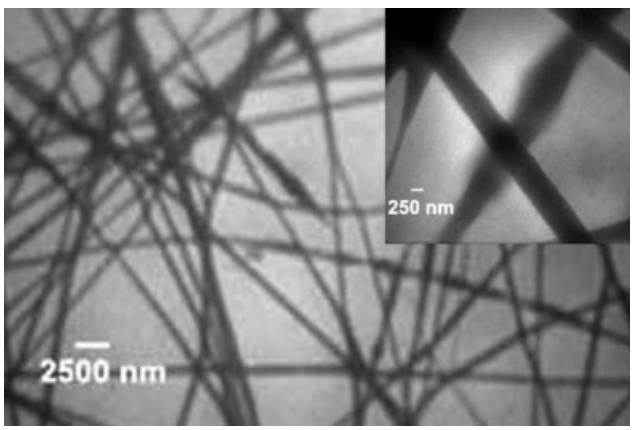


**Figure 3** TEM micrographs of the nanofibers produced in Experiment D4.

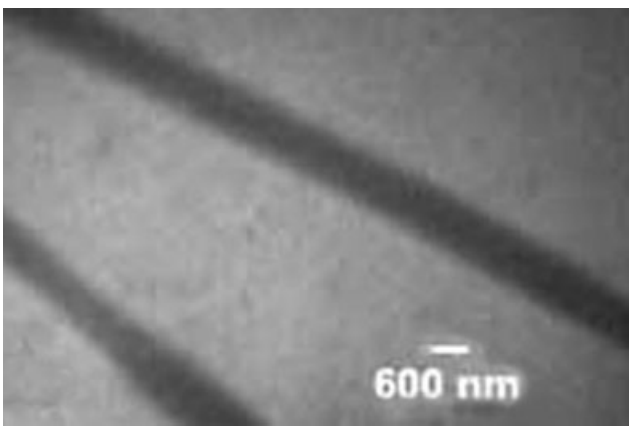


**Figure 5** TEM micrograph of the nanofibers produced in Experiment N.

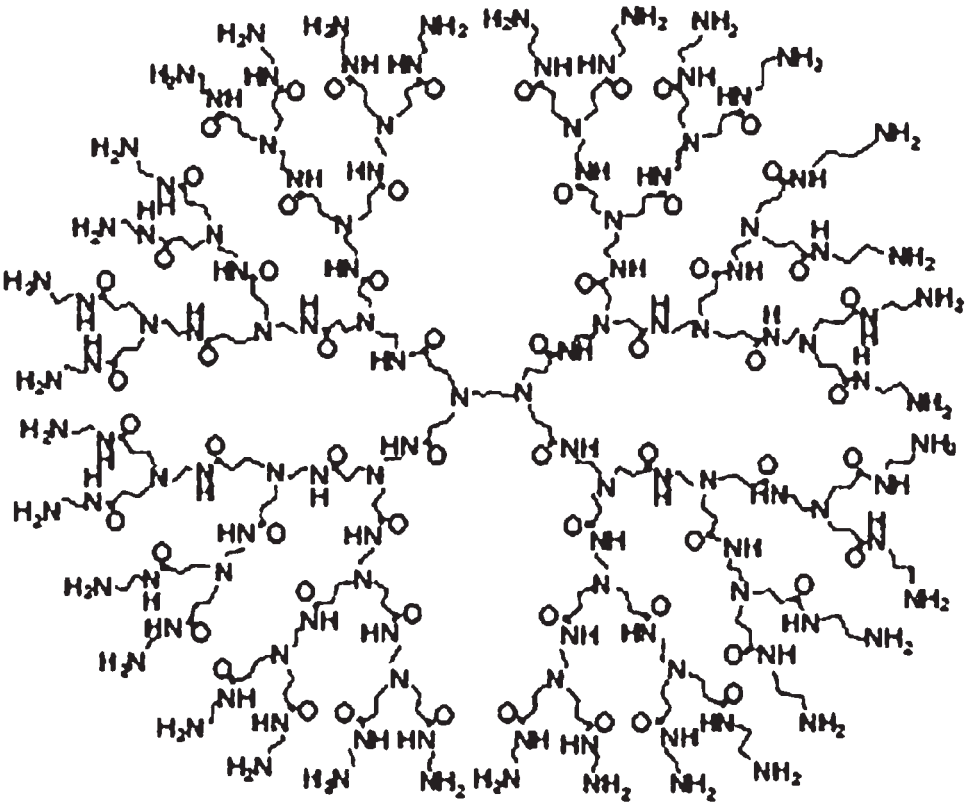

**Figure 6** Chemical structure of the used PAMAM.

tendency toward aggregation in dendrimers, which has been reported in other work;[26–30] in this case, aggregation appears to take place in the composite dendrimeric–polymeric system, leading to such aureole morphology. This segregation is greatly influenced by the crystallization of the PEO, and crystallinity is likely to be the driving force for phase segregation and dendrimer migration in such a

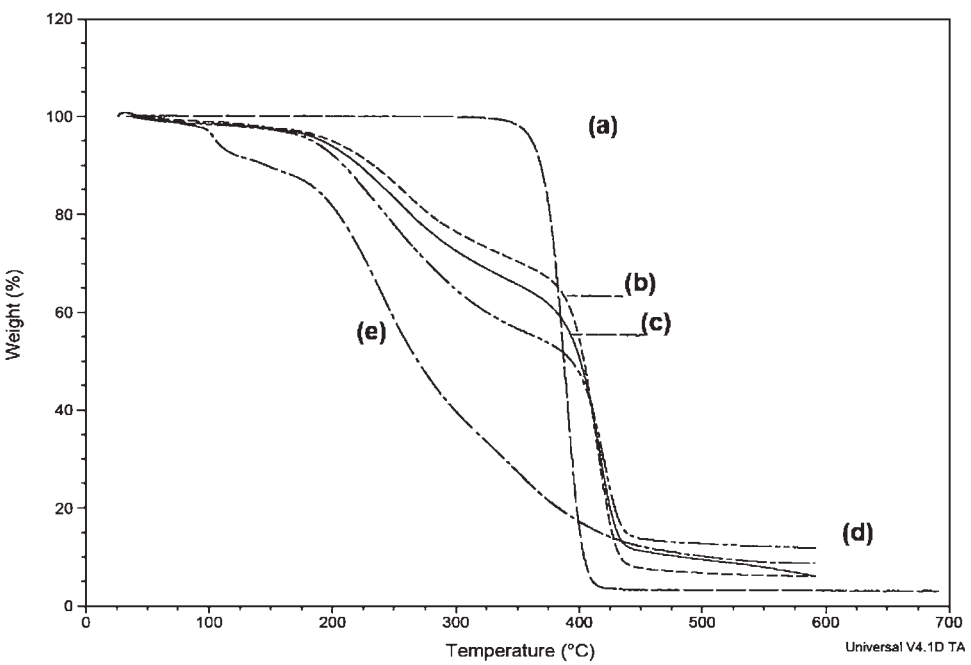


**Figure 7** TGA thermographs of the nanofibers produced in experiments (a) N, (b) D5, (c) D4, (d) D2, and (e) pure PAMAM.

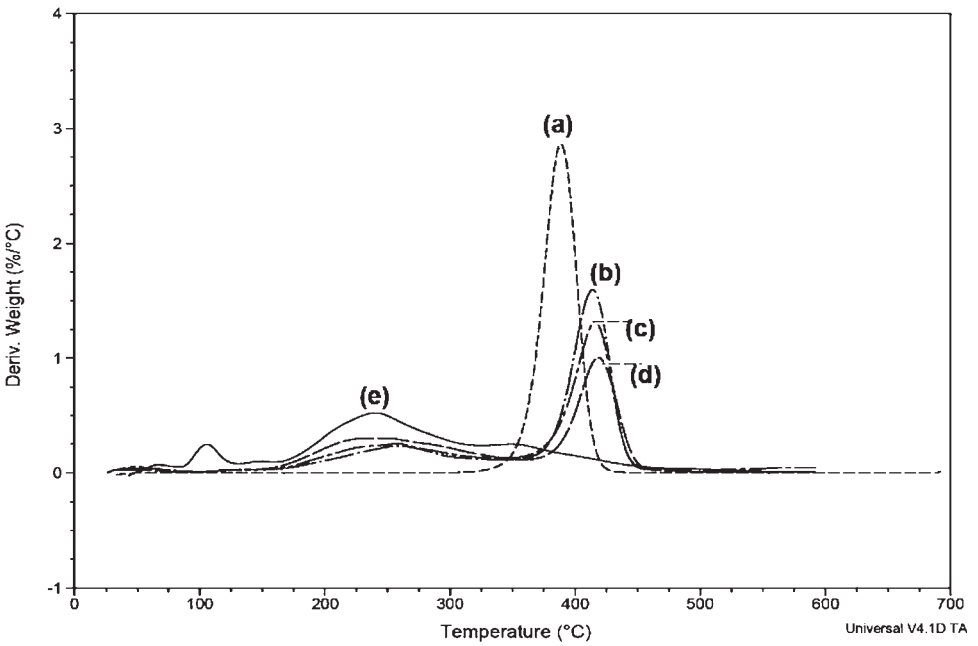


**Figure 8** DTGA thermographs of the nanofibers produced in experiments (a) N, (b) D5, (c) D4, (d) D2, and (e) pure PAMAM.

composite. In fact, dendrimer segregation during fiber formation is driven by the presence of the PEO chains that can be crystallized.

This aureole morphology increases the diameter of the nanofibers as shown in Figure 1 by up to 1300 nm and produces two different regions with different density. Because G3 PAMAM size is about 1.5 nm, the number of dendrimers that are responsible for such an increase in fiber diameter can be estimated (considering phase mixing).

TGA analysis was also conducted to confirm the existence of PAMAM dendrimer in the fiber mat. Figures 7 and 8 present the TGA and DTGA thermographs of the fiber mats. The Curves (a–d) in Figure 7 are TGA thermographs of fiber mats obtained in experiments N, D5, D4, and D2, respectively, and pure PAMAM (Curve e). As shown in this figure, Curve (a) shows just one weight loss at about 340–430°C, which is related to the PEO decomposition. In Curves (b–d), there are two weight losses, which overlap and are related to the decomposition of PAMAM (at about 160–500°C) and of PEO. In Curve (e), there is a weight loss at about 120°C, which is related to the water absorbed within the PAMAM dendrimer, but there is no such a peak in TGA of produced fibers due to the evaporation of water during electrospinning.

The comparison of Curves (b) and (c) in Figure 7 shows that the two products have the same polymer decomposition but Curve (c) (the TGA thermograph of the D4 fibers) has a higher decomposition percentage in the range of 160–340°C than D5 fibers, which is related to higher amounts of PAMAM dendrimer within the D4 fibers. Because the used PAMAM decomposes at about 160–500°C, we can conclude that the second weight loss which started at 160°C in Curves (b)–(e) (Fig. 8) is due to the decomposition of PAMAM in the fiber. Thus, this weight loss in the TGA thermograph shows the existence of PAMAM dendrimer in the PEO fibers.

Thermal properties of the fiber mats produced in these experiments (Exp. D5, D4, D3 and D2) were also analyzed by DSC analysis. The DSC thermographs of these experiments are given in Figure 9. Curves (b)–(e) in this figure are DSC thermographs of fiber mats obtained in Experiments D2, D3, D4, and D5, respectively, and Curve (a) is the DSC

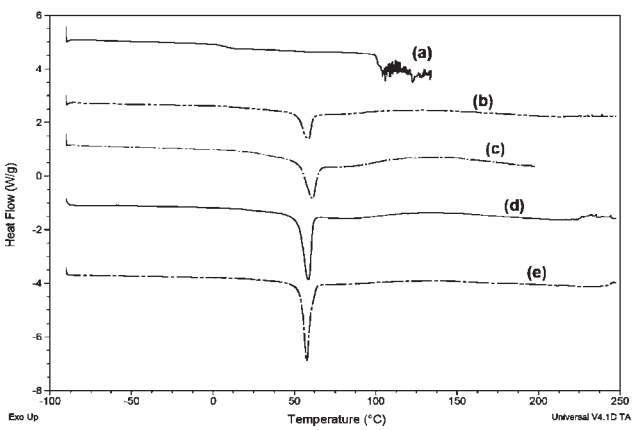


**Figure 9** DSC thermographs of the nanofibers produced in experiments (a) pure PAMAM, (b) D2, (c) D3, (d) D4, and (e) D5.

**TABLE II**
**Thermal Properties of Produced Nanofibers**

| Experiment | Melting point (°C) | Heat of fusion $\Delta H_{total}$ (J/g) | Crystallinity (%) | First thermal decomposition temperature | Second thermal decomposition temperature | Residue at 600°C obtained by TGA (%) |
|---|---|---|---|---|---|---|
| Exp. N | 59.10 | 128.80 | 60 | – | 388 | 2.80 |
| Exp. D5 | 54.00 | 95.34 | 63 | 258 | 414 | 7.19 |
| Exp. D4 | 52.79 | 85.60 | 66 | 257 | 417 | 8.40 |
| Exp. D3 | 53.48 | 57.87 | 54 | –[b] | –[b] | –[b] |
| Exp. D2 | 52.62 | 39.05 | 45 | 254 | 420 | 13.44 |
| Pure PAMAM[a] | – | – | – | 241 | – | 10.32 |

[a] PAMAM cannot be electrospun alone.
[b] Not obtained in this work.

thermograph of pure PAMAM, which started to lose its absorbed water at about 120°C.

The melting points and the percentage of crystallinity ($X_c$%) of the products in the experiments were obtained from the DSC analyses and are listed in Table II.

The specific heat of crystallization of the nanocomposite $\Delta H_{comp}$ was calculated using the following formula:

$$\Delta H_{comp} = [\Delta H_{total} \times 100]/y$$

where $\Delta H_{total}$ is obtained from the peak area of the DSC curve (j/g), and $y$ is the concentration of PEO (wt %). The given crystallinities ($X_c$%) of the nanofiber mats in Table II were calculated using the equation $X_c\% = [\Delta H_{comp} / \Delta H_f^0] \times 100$, where $\Delta H_f^0$ is the heat of fusion of completely crystalline PEO (that is 213.7 J/g)[31] and $\Delta H_{comp}$ is the heat of fusion for the sample calculated from the former equation. As shown in Figure 9 and Table II, the melting point and the crystallinity of pure PEO fibers (Exp. N) are higher than those of PEO fibers having PAMAM dendrimer at high-dendrimer concentration within fibers. At high-PAMAM loading within fibers, the crystallinity reduces sharply. Because one of the factors responsible for the production of such aureole morphology is crystallinity of semicrystalline PEO, higher PEO-PAMAM phase mixing can be obtained at lower PEO crystallinity.

The data given in Table II also show that the crystallinity of the fibers produced is higher in Exp. D4 than in Exp. D3. The DSC thermograph shows one phase changes in the range of 35–70°C, which is related to PEO melting. The aforementioned results are summarized in Table II and show the reduction of PEO crystallinity by adding the PAMAM dendrimer from 60% for pure PEO nanofibers to 54% for D3 nanofibers and 45% for D2 nanofibers.

All of the results obtained by the aforementioned analyses elucidate the ability of electrospinning to produce aureole morphology nanofibers.

Here, the PEO nanofibers, a model of fibers, were chosen for practical and theoretical analysis. Further consideration leads us to investigate whether other polymer solutions could be electrospun with PAMAM dendrimer.

## CONCLUSION

Polymeric–dendrimeric composite aureole nanofibers were produced through electrospinning. The nanofibers with 400–1300 nm in diameter were produced via electrospinning of PEO solution having PAMAM dendrimer, and the existence of PAMAM in the nanofibers was proven by TEM and TGA analyses. The amounts of dendrimer within the fibers decrease by the decreases in the PAMAM concentration in starting solution and as a consequence, the nanofibers that have the maximal amounts of PAMAM dendrimer show aureole morphology in more regions with a larger aureole diameter. The crystallinity of PEO, shown by DSC analyses, was reduced in electrospinning process in the presence of PAMAM dendrimer at high-PAMAM loading.

The authors thank Mr. Hashemi for providing TEM micrographs from the Laboratory of Electronic Microscopy of University College of Science in the University of Tehran. They also thank Ms. Fotouhi.

## References

1. McCann, J. T.; Li, D.; Xia, Y. J Mater Chem 2005, 15, 735.
2. Faridi-Majidi, R.; Sharifi-Sanjani, N.; Madani, M. J Nanosci Nanotechnol 2008, 8, 2627.
3. Chronakis, I. S. J Mater Process Technol 2005, 167, 283.
4. Yarin, A. L.; Zussman, E.; Wendorff, J. H.; Greiner, A. J Mater Chem 2007, 17, 2585.
5. Dror, Y.; Salalha, W.; Khalfin, R. L.; Cohen, Y.; Yarin, A. L.; Zussman, E. Langmuir 2003, 19, 7012.
6. Ko, F.; Gogotsi, Y.; Ali, A.; Naguib, N.; Ye, H.; Yang, G.; Li, C.; Willis, P. Adv Mater 2003, 15, 1161.
7. Dror, Y.; Khalfin, R. L.; Cohen, Y.; Yarin, A. L.; Zussman, E. Langmuir 2004, 20, 9852.

8. Lim, J.; Lee, C.; Kim, S.; Kim, I.; Kim, S. J Macromol Sci Pure Appl Chem 2006, 43, 785.
9. Nuansing, W.; Ninmuang, S.; Jarernboon, W.; Maensiri, S.; Seraphin, S. Mater Sci Eng B 2006, 131, 147.
10. Lee, D. Y.; Kim, B.-Y.; Lee, S.-J.; Lee, M.-H.; Song, Y.-S.; Lee, J.-Y. J. Korean Phys Soc 2006, 48, 1686.
11. Watthanaarun, J.; Pavarajarn, V.; Supaphol, P. Sci Technol Adv Mater 2005, 6, 240.
12. Tomalia, D. A.; Baker, H.; Dewald, J.; Hall, M.; Kallos, G.; Martin, S.; Roeck, J.; Ryder, J.; Smith, P. Polym J 1984, 17, 117.
13. Prosa, T. J.; Bauer, B. J.; Amis, E. J.; Tomalia, D. A.; Scherrenberg, R. J Polym Sci 1997, 35, 2913.
14. Imae, T.; Funayama, K.; Aoi, K.; Tsutsumiuchi, K.; Okada, M.; Furusaka, M. Langmuir 1999, 15, 4076.
15. Lee, I.; Athey, B. D.; Wetzel, A. V.; Meixner, W. Macromolecules 2002, 35, 4510.
16. Ghosh, S. K.; Kawaguchi, S.; Jinbo, Y.; Izumi, Y.; Yamaguchi, K.; Taniguchi, T.; Nagai, K.; Koyama, K. Macromolecules 2003, 36, 9162.
17. Funayama, K.; Imae, T.; Seto, H.; Aoi, K.; Tsutsumiuchi, K.; Okada, M.; Nagao, M.; Furusaka, M. J Phys Chem B 2003, 107, 1353.
18. Funayama, K.; Imae, T.; Aoi, K.; Tsutsumiuchi, K.; Okada, M.; Furusaka, M.; Nagao, M. J Phys Chem B 2003, 107, 1532.
19. Hedden, R. C.; Bauer, B. J. Macromolecules 2003, 36, 1829.
20. Lin, W.; Galletto, P.; Borkovec, M. Langmuir 2004, 20, 7465.
21. Kovvali, A. S.; Chen, H.; Sirkar, K. K. J Am Chem Soc 2000, 122, 7594.
22. Kovvali, A. S.; Sirkar, K. K. Ind Eng Chem Res 2001, 40, 2502.
23. Tomalia, D. A. B. V.; Hall, M.; Hedstrand, D. M. Macromolecules 1987, 20, 1164.
24. Iyer, J.; Hammond, P. T. Langmuir 1999, 15, 1299.
25. Iyer, J. Doctoral Dissertation, Chemical Engineering Department, Massachusetts Institute of Technology, Cambridge, MA, 1999.
26. Johnson, M. A.; Santini, C. M. B.; Iyer, J.; Satija, S.; Ivkov, R.; Hammond, P. T. Macromolecules 2002, 35, 231.
27. Aoi, K.; Motoda, A.; Okada, M. Macromol Rapid Commun 1997, 18, 945.
28. Chapman, T. M.; Hillyer, G. L.; Mahan, E. J.; Shaffer, K. A. J Am Chem Soc 1994, 116, 11195.
29. van Hest, J. C. M.; Baars, M. W. P. L.; Elissen-Roman, C.; van Genderen, M. H. P.; Meijer, E. W. Macromolecules 1995, 28, 6689.
30. van Hest, J. C. M.; Delnoye, D. A. P.; Baars, M. W. P. L.; van Genderen, M. H. P.; Meier, E. W. Science 1995, 268, 1592.
31. Xi, J.; Tang, X. Chem Phys Lett 2004, 393, 271.